

First magnetic field models for recently discovered magnetic β Cephei and slowly pulsating B stars¹

S. Hubrig, I. Ilyin

Astrophysikalisches Institut Potsdam, An der Sternwarte 16, 14482 Potsdam, Germany

shubrig@aip.de

M. Schöller

European Southern Observatory, Karl-Schwarzschild-Str. 2, 85748 Garching bei München, Germany

M. Briquet

Instituut voor Sterrenkunde, Katholieke Universiteit Leuven, Celestijnenlaan 200 D, 3001 Leuven, Belgium

T. Morel

Institut d'Astrophysique et de Géophysique, Université de Liège, Allée du 6 Août, Bât. B5c, 4000 Liège, Belgium

P. De Cat

Koninklijke Sterrenwacht van België, Ringlaan 3, 1180 Brussel, Belgium

ABSTRACT

In spite of recent detections of magnetic fields in a number of β Cephei and slowly pulsating B (SPB) stars, their impact on stellar rotation, pulsations, and element diffusion is not sufficiently studied yet. The reason for this is the lack of knowledge of rotation periods, the magnetic field strength distribution and temporal variability, and the field geometry. New longitudinal field measurements of four β Cephei and candidate β Cephei stars, and two SPB stars were acquired with FORS 2 at the VLT. These measurements allowed us to carry out a search for rotation periods and to constrain the magnetic field geometry for four stars in our sample.

Subject headings: stars: early-type — stars: magnetic field — stars: oscillations — stars: variables: general — stars: fundamental parameters — stars: individual (ξ^1 CMa, 15 CMa, α Pyx, ϵ Lup, 33 Eri, HY Vel)

¹Based on observations obtained at the European Southern Observatory (ESO programme 084.D-0230(A)).

1. Introduction

For several years, a magnetic field survey of main-sequence pulsating B-type stars, namely the slowly pulsating B (SPB) stars and β Cephei stars, has been undertaken by our team with FORS 1 in spectropolarimetric mode at the VLT, allowing us to detect in four β Cephei stars and in 16 slowly pulsating B stars, for the first time, longitudinal magnetic fields of the order of a few hundred Gauss (Hubrig et al. 2006, 2009). β Cephei variables have spectral types B0–B2 and pulsate in low-order pressure and gravity modes with periods between 2 and 6 hours. Slowly pulsating B (SPB) stars are mid-B type (B3–B9) objects pulsating in high-order gravity modes with periods in the range of 0.5–3 days. Pulsating stars are currently considered as promising targets for asteroseismic analysis (e.g. Shibahashi & Aerts 2000), which requires as input the observed parameters of the magnetic field topology. Early magnetic field searches of β Cephei stars were mostly unsuccessful due to low precision (see Babcock 1958; Rudy & Kemp 1978). Before we started our systematic search for magnetic fields in pulsating B-type stars, a weak magnetic field was detected in two β Cephei stars, in the prototype of the class, β Cep itself, by Henrichs et al. (2000) and in V2052 Oph by Neiner et al. (2003a). The first detection of a weak magnetic field in the SPB star ζ Cas was reported by Neiner et al. (2003b). The detected magnetic objects for which we gathered several magnetic field measurements showed a field that varies in time, but no periodicity could be derived yet due to the limited amount of VLT observing time. Among these targets with a detected magnetic field, we selected two slowly pulsating B stars, two β Cephei stars, and two candidate β Cephei stars with suitable coordinates, for successive VLT multi-epoch magnetic measurements. The list of the selected targets is presented in Table 1. In the four columns we list the HD number, another identifier, the spectral type retrieved from the SIMBAD database, the pulsating type, and membership in a spectroscopic binary system. An asterisk in front of the HD number denotes candidate β Cephei stars (cf. Stankov & Handler 2005). This most recent study aimed at the determination of magnetic field properties for these stars, such as field strength, field geometry, and time variability. Here we present the results of 62 new magnetic field measurements

Table 1: The observed β Cephei and SPB stars.

| HD | Other Identifier | Spectral Type | Comments |
|----------|---------------------|------------------|-----------------|
| 24587 | 33 Eri | B5V | SPB, SB1 |
| 46328 | ξ^1 CMa | B1III | β Cep |
| 50707 | 15 CMa | B1Ib | β Cep |
| * 74575 | α Pyx | B1.5III | β Cep |
| 74560 | HY Vel | B3IV | SPB, SB1 |
| * 136504 | ϵ Lup | B2IV-V | β Cep, SB |

of the six selected stars and discuss the obtained results on their rotation periods and magnetic field geometry.

2. Magnetic field measurements and period determination

Multi-epoch time series of polarimetric spectra of the pulsating stars were obtained with FORS 2² on Antu (UT1) from 2009 September to 2010 March in service mode. Using a slit width of 0".4, the achieved spectral resolving power of FORS 2 obtained with the GRISM 600B was about 2000. A detailed description of the assessment of the longitudinal magnetic field measurements using FORS 2 is presented in our previous papers (e.g., Hubrig et al. 2004a,b, and references therein). The mean longitudinal magnetic field, $\langle B_z \rangle$, was derived using

$$\frac{V}{I} = -\frac{g_{\text{eff}} e \lambda^2}{4\pi m_e c^2} \frac{1}{I} \frac{dI}{d\lambda} \langle B_z \rangle, \quad (1)$$

where V is the Stokes parameter which measures the circular polarisation, I is the intensity in the unpolarised spectrum, g_{eff} is the effective Landé factor, e is the electron charge, λ is the wavelength, m_e the electron mass, c the speed of light, $dI/d\lambda$ is the derivative of Stokes I , and $\langle B_z \rangle$ is the mean longitudinal magnetic field. The measurements of the longitudinal magnetic field were carried out in two ways, using the whole spectrum ($\langle B_z \rangle_{\text{all}}$) and using only the hydrogen lines ($\langle B_z \rangle_{\text{hyd}}$).

Two additional polarimetric spectra of ξ^1 CMa were obtained with the SOFIN spectrograph installed at the 2.56 m Nordic Optical Telescope on La Palma, one on 2008 September 13, and another one on 2010 January 01. SOFIN (Tuominen et al. 1999) is a high-resolution echelle spectrograph mounted at the Cassegrain focus of the NOT. The star was observed with the low-resolution camera with $R = \lambda/\Delta\lambda \approx 30\,000$. We used the 2K Loral CCD detector to register 40 echelle orders partially covering the range from 3500 to 10 000 Å with a length of the spectral orders of about 140 Å. Two such exposures with quarter-wave plate angles separated by 90° are necessary to derive circularly polarised spectra. The spectra were reduced with the 4A software package (Ilyin 2000).

A frequency analysis was performed on the longitudinal magnetic field measurements $\langle B_z \rangle_{\text{all}}$ (which generally show smaller sigmas) available from our previous (Hubrig et al. 2006, 2009) and the current studies using a non-linear least-squares fit of the multiple harmonics utilizing the Levenberg-Marquardt method (Press et al. 1992) with an optional possibility of pre-whitening the trial harmonics. To detect the most probable period, we calculated the frequency spectrum for the same harmonic with a number of trial frequencies by solving the linear least-squares problem. At

²The spectropolarimetric capabilities of FORS 1 were moved to FORS 2 in 2009.

Table 2: Magnetic field measurements of β Cephei stars with FORS 1/2 and SOFIN (marked with an asterisk). All quoted errors are 1σ uncertainties.

| MJD | Rotation Phase | $\langle B_z \rangle_{\text{all}}$ [G] | $\langle B_z \rangle_{\text{hyd}}$ [G] |
|----------------|-------------------|---|---|
| ξ^1 CMa | | | |
| 53475.046 | 0.702 | 282 \pm 42 | 280 \pm 44 |
| 53506.971 | 0.351 | 278 \pm 43 | 330 \pm 45 |
| 54061.325 | 0.715 | 287 \pm 42 | 360 \pm 45 |
| 54107.266 | 0.795 | 312 \pm 43 | 319 \pm 46 |
| 54114.028 | 0.898 | 309 \pm 35 | 347 \pm 38 |
| 54114.182 | 0.969 | 364 \pm 35 | 382 \pm 47 |
| 54116.108 | 0.853 | 307 \pm 45 | 276 \pm 58 |
| 54155.086 | 0.738 | 308 \pm 47 | 349 \pm 35 |
| 54343.371 | 0.132 | 345 \pm 11 | 379 \pm 15 |
| 54345.338 | 0.034 | 366 \pm 11 | 400 \pm 12 |
| 54345.414 | 0.069 | 340 \pm 11 | 378 \pm 18 |
| 54548.982 | 0.476 | 277 \pm 55 | 297 \pm 87 |
| 54549.995 | 0.941 | 380 \pm 37 | 332 \pm 55 |
| *54722.274 | 0.991 | 386 \pm 39 | |
| 55107.342 | 0.678 | 229 \pm 30 | 302 \pm 44 |
| 55109.325 | 0.589 | 206 \pm 31 | 233 \pm 52 |
| 55113.224 | 0.378 | 203 \pm 44 | 320 \pm 65 |
| 55135.200 | 0.461 | 213 \pm 39 | 240 \pm 59 |
| 55150.342 | 0.409 | 176 \pm 51 | 322 \pm 76 |
| 55153.340 | 0.784 | 295 \pm 61 | 470 \pm 94 |
| 55159.329 | 0.532 | 207 \pm 29 | 254 \pm 41 |
| 55163.085 | 0.256 | 282 \pm 35 | 389 \pm 56 |
| 55164.092 | 0.718 | 272 \pm 45 | 416 \pm 88 |
| 55165.106 | 0.183 | 301 \pm 39 | 431 \pm 64 |
| 55168.091 | 0.553 | 232 \pm 44 | 174 \pm 59 |
| *55201.279 | 0.781 | 297 \pm 26 | |
| α Pyx | | | |
| 54082.341 | 0.816 | 142 \pm 48 | 219 \pm 60 |
| 54109.150 | 0.200 | 132 \pm 50 | 184 \pm 60 |
| 55107.378 | 0.362 | 5 \pm 31 | –29 \pm 48 |
| 55118.347 | 0.792 | 120 \pm 28 | 89 \pm 34 |
| 55120.351 | 0.418 | –14 \pm 26 | –35 \pm 44 |
| 55168.167 | 0.371 | 24 \pm 39 | –26 \pm 68 |
| 55171.162 | 0.308 | 40 \pm 45 | 42 \pm 69 |
| ϵ Lup | | | |
| 54344.998 | | –156 \pm 34 | –128 \pm 36 |
| 55225.268 | | –130 \pm 94 | –191 \pm 129 |
| 55226.272 | | –33 \pm 39 | –40 \pm 52 |
| 55227.285 | | –104 \pm 44 | –185 \pm 69 |
| 55228.324 | | –7 \pm 42 | 7 \pm 51 |
| 55258.206 | | –147 \pm 46 | –162 \pm 54 |
| 55259.260 | | –105 \pm 41 | –158 \pm 66 |
| 15 CMa | | | |
| 54107.318 | 0.085 | 163 \pm 52 | 157 \pm 58 |
| 54345.372 | 0.917 | 149 \pm 19 | 123 \pm 27 |
| 55107.326 | 0.192 | 86 \pm 26 | 113 \pm 55 |
| 55109.371 | 0.354 | –41 \pm 36 | –130 \pm 52 |
| 55112.380 | 0.592 | –92 \pm 48 | –88 \pm 74 |
| 55150.330 | 0.594 | –75 \pm 54 | –49 \pm 78 |
| 55159.295 | 0.304 | 35 \pm 34 | 13 \pm 51 |
| 55163.101 | 0.605 | –25 \pm 39 | –45 \pm 58 |
| 55164.104 | 0.684 | 31 \pm 49 | –24 \pm 61 |
| 55165.118 | 0.764 | 76 \pm 41 | 19 \pm 60 |
| 55168.104 | 0.000 | 128 \pm 42 | 126 \pm 65 |
| 55170.090 | 0.158 | 138 \pm 52 | 90 \pm 120 |
| 55171.133 | 0.240 | 21 \pm 42 | –12 \pm 67 |
| 55173.143 | 0.399 | –58 \pm 88 | –64 \pm 122 |
| 55177.323 | 0.730 | 7 \pm 33 | 0 \pm 62 |

Table 3: Magnetic field measurements of SPB stars with FORS 1/2. All quoted errors are 1σ uncertainties.

| MJD | Rotation Phase | $\langle B_z \rangle_{\text{all}}$ [G] | $\langle B_z \rangle_{\text{hyd}}$ [G] |
|-----------|-------------------|---|---|
| 33 Eri | | | |
| 52971.071 | 0.599 | -122 ± 64 | -120 ± 68 |
| 53574.415 | 0.157 | -14 ± 33 | -16 ± 36 |
| 53630.250 | 0.796 | -34 ± 27 | -32 ± 29 |
| 54086.175 | 0.135 | -30 ± 54 | -45 ± 61 |
| 54343.301 | 0.098 | 67 ± 60 | 83 ± 65 |
| 55107.154 | 0.105 | 116 ± 39 | 166 ± 49 |
| 55108.197 | 0.929 | -25 ± 43 | -43 ± 56 |
| 55109.350 | 0.822 | 5 ± 35 | 10 ± 49 |
| 55110.181 | 0.471 | -98 ± 48 | -138 ± 70 |
| 55111.222 | 0.284 | -39 ± 45 | -52 ± 69 |
| 55112.347 | 0.164 | 0 ± 43 | -20 ± 72 |
| 55113.188 | 0.821 | 25 ± 44 | 62 ± 73 |
| 55120.099 | 0.223 | -63 ± 55 | -177 ± 79 |
| 55135.184 | 0.013 | 90 ± 52 | 112 ± 64 |
| 55149.176 | 0.948 | 117 ± 37 | 119 ± 44 |
| 55150.302 | 0.829 | 12 ± 46 | -7 ± 72 |
| 55161.089 | 0.259 | -126 ± 46 | -168 ± 55 |
| 55163.031 | 0.777 | -41 ± 44 | -18 ± 59 |
| HY Vel | | | |
| 53002.141 | | -180 ± 57 | -199 ± 61 |
| 53143.986 | | -48 ± 60 | -53 ± 66 |
| 54108.348 | | -198 ± 55 | -191 ± 58 |
| 55107.361 | | 34 ± 59 | -61 ± 79 |
| 55112.367 | | -25 ± 51 | -58 ± 69 |
| 55118.320 | | 133 ± 62 | 162 ± 83 |
| 55120.324 | | 63 ± 33 | 59 ± 48 |
| 55168.150 | | -99 ± 38 | -147 ± 64 |
| 55169.349 | | 47 ± 41 | 78 ± 73 |
| 55171.150 | | 40 ± 59 | -11 ± 88 |
| 55173.269 | | 17 ± 51 | -19 ± 68 |
| 55177.341 | | 117 ± 35 | 160 ± 49 |
| 55181.141 | | 42 ± 36 | 35 ± 54 |
| 55182.280 | | 67 ± 38 | 144 ± 53 |
| 55189.176 | | 19 ± 44 | 30 ± 68 |

each trial frequency we performed a statistical test of the null hypothesis for the absence of periodicity (Seber 1977), i.e. testing that all harmonic amplitudes are at zero. The resulting F-statistics can be thought of as the total sum including covariances of the ratio of harmonic amplitudes to their standard deviations, i.e. as a signal-to-noise ratio (Ilyin 2000). The F-statistics allows to derive the false alarm probability of the trial period based on the F-test (Press et al. 1992). Periodicity was found for four out of the studied six stars. The derived ephemeris for the detected periods are

$$\begin{aligned}
\xi^1 \text{ CMa} : \langle V\&I \rangle^{\max} &= \text{MJD}55140.73332 \pm 0.03794 + 2.17937 \pm 0.00012E \\
15 \text{ CMa} : \langle V\&I \rangle^{\max} &= \text{MJD}55168.09911 \pm 0.16667 + 12.64115 \pm 0.00822E \\
\alpha \text{ Pyx} : \langle V\&I \rangle^{\max} &= \text{MJD}55144.59481 \pm 0.04105 + 3.19779 \pm 0.00019E \\
33 \text{ Eri} : \langle V\&I \rangle^{\max} &= \text{MJD}55123.65285 \pm 0.03243 + 1.27947 \pm 0.00005E
\end{aligned}$$

The logbook of the new FORS 2 and the old, revisited, FORS 1 spectropolarimetric observations is presented in Tables 2 and 3. In the first column we indicate the MJD value at mid exposure. The phases of the measurements of the magnetic field, if available, are listed in Column 2. In Columns 3 and 4 we present the longitudinal magnetic field $\langle B_z \rangle_{\text{all}}$ measured using the whole spectrum and the longitudinal magnetic field $\langle B_z \rangle_{\text{hyd}}$ using only the hydrogen lines. Phase diagrams of the data folded with the determined periods are presented in Fig. 1. The quality of our fits is described by a reduced χ^2 -value which appears in the four panels of Fig. 1.

3. Characterisation of the magnetic field geometry for the stars with determined periods

The determination of the fundamental parameters and the description of the pulsating properties of all studied stars were presented by Hubrig et al. (2009, Tables 1a, 1b, and 4). The most

Table 4: Magnetic field models for the stars with detected periods.

| Object | | $\xi^1 \text{ CMa}$ | 15 CMa | $\alpha \text{ Pyx}$ | 33 Eri |
|---------------------------|-----------------|---------------------|------------------|----------------------|------------------|
| $\langle B_z \rangle$ | [G] | 281.6 \pm 4.3 | 45.3 \pm 7.1 | 90.3 \pm 5.1 | −44.1 \pm 15.3 |
| $A_{\langle B_z \rangle}$ | [G] | 80.3 \pm 5.8 | 116.3 \pm 12.1 | 119.7 \pm 12.8 | 112.0 \pm 25.5 |
| $v \sin i$ | [km s $^{-1}$] | 9 \pm 2 | 34 \pm 4 | 11 \pm 2 | 25 \pm 4 |
| R | [R $_{\odot}$] | 7.1 \pm 0.9 | 10.0 \pm 1.5 | 6.3 \pm 1.0 | 2.5 \pm 0.3 |
| v_{eq} | [km s $^{-1}$] | 165 \pm 21 | 40 \pm 6 | 100 \pm 16 | 99 \pm 12 |
| i | [$^{\circ}$] | 3.1 \pm 0.8 | 58.1 \pm 17.6 | 6.3 \pm 1.5 | 14.6 \pm 3.0 |
| β | [$^{\circ}$] | 79.1 \pm 2.8 | 57.9 \pm 18.3 | 85.2 \pm 1.3 | 84.1 \pm 2.7 |
| B_d | [G] | 5300 \pm 1100 | 570 \pm 50 | 3800 \pm 500 | 1500 \pm 350 |

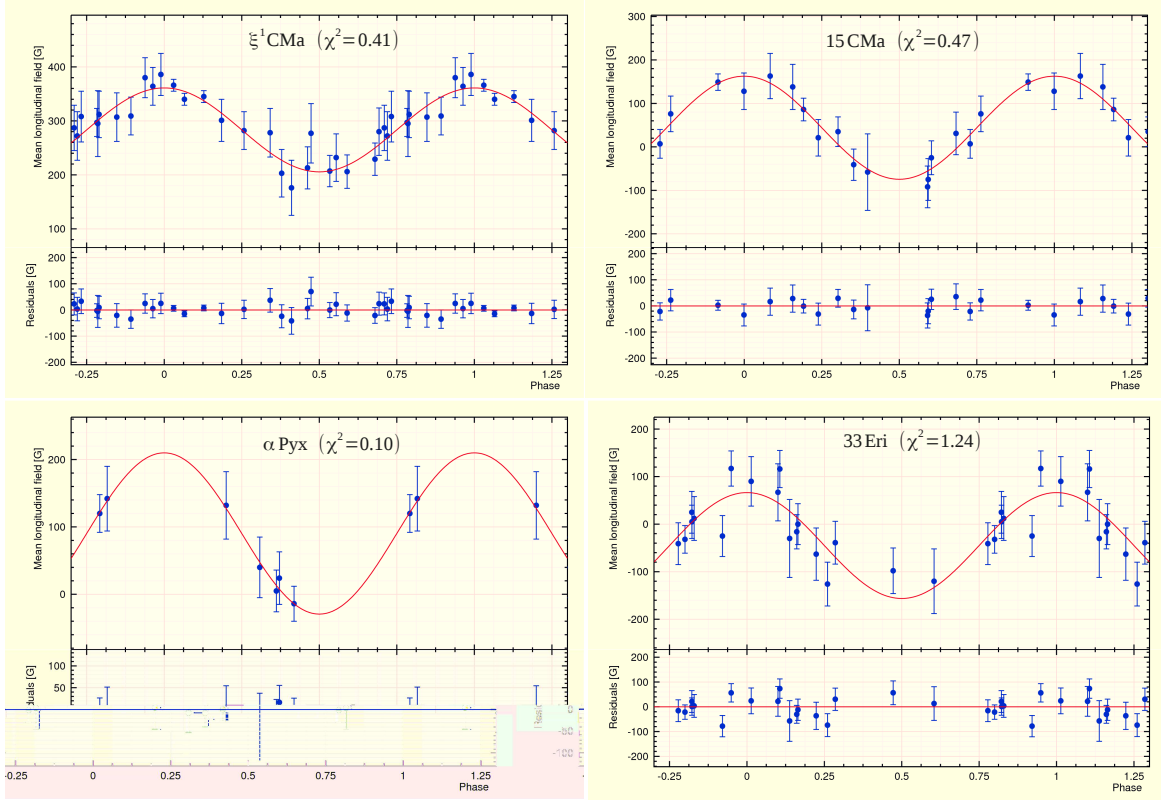


Fig. 1.— Phase diagrams with the best sinusoidal fit for the longitudinal magnetic field measurements. The residuals (Observed – Calculated) are shown in the lower panels. The deviations are mostly of the same order as the error bars, and no systematic trends are obvious, which justifies a single sinusoid as a fit function.

simple modeling of the magnetic field geometry is based on the assumption that the studied stars are oblique dipole rotators, i.e. their magnetic field can be approximated by a dipole with the magnetic axis inclined to the rotation axis.

The magnetic dipole axis tilt β is constrained by

$$r = \frac{\langle B_z \rangle^{\min}}{\langle B_z \rangle^{\max}} = \frac{\cos \beta \cos i - \sin \beta \sin i}{\cos \beta \cos i + \sin \beta \sin i}, \quad (2)$$

so that the obliquity angle β is given by

$$\beta = \arctan \left[\left(\frac{1-r}{1+r} \right) \cot i \right]. \quad (3)$$

In Table 4 we show for each star with detected periodicity in Rows 2 and 3 the mean value $\overline{\langle B_z \rangle}$ and the amplitude of the field variation $A_{\langle B_z \rangle}$. In Row 4 we present $v \sin i$ values published recently by Lefever et al. (2010) for ξ^1 CMa and 15 CMa and from Hubrig et al. (2009) for α Pyx and 33 Eri. The radius values in Row 5 were taken from Hubrig et al. (2009). The radius of 15 CMa ($R=10.0 \pm 1.5 R_\odot$) was derived in the same way as in Hubrig et al. (2009) by adopting the values of T_{eff} and $\log g$ from Lefever et al. (2010). In the last four rows we list the v_{eq} and the parameters of the magnetic field dipole models. The polar field strength B_d in the last row was calculated following Preston (1969) using limb darkening parameters from Diaz-Cordovés et al. (1995).

4. Discussion

Using FORS 1/2 and SOFIN longitudinal magnetic field measurements collected in our recent studies, we were able to determine rotation periods and constrain the field geometry of two β Cephei stars, one candidate β Cephei star, and one SPB star. The dipole model provides a satisfactory fit to the data and among the very few presently known magnetic β Cephei stars, ξ^1 CMa and α Pyx possess the largest magnetic fields, with a dipole strength of several kG. Briquet et al. (2007) discussed the position of SPB and chemically peculiar Bp stars in the H-R diagram, indicating that the group of Bp stars is significantly younger than the group of SPB stars. A similar conclusion was deduced by Hubrig et al. (2007), who studied the evolution of magnetic fields in Ap and Bp stars with definitely determined magnetic field geometries across the main sequence. The vast majority of Bp stars exhibits a smooth, single-wave variation of the longitudinal magnetic field during the stellar rotation cycle. These observations are considered as evidence for a dominant dipolar contribution to the magnetic field topology. It is of interest that the study of Hubrig et al. (2007) indicates the prevalence of larger obliquities β , namely $\beta > 60^\circ$, in more massive stars. The

magnetic field models for the three β Cephei stars and the one SPB star presented in this work confirm this trend.

The insufficient knowledge of the strength, geometry, and time variability of magnetic fields in hot pulsating stars prevented until now important theoretical studies on the impact of magnetic fields on stellar rotation, pulsations, and element diffusion. Although it is expected that the magnetic field can distort the frequency patterns (e.g. Hasan et al. 2005), such a perturbation is not yet detected in hot pulsating stars. Splitting of non-radial pulsation modes was observed for 15 CMa (Shobbrook et al. 2006), but the identification of these modes is still pending. The magnetic β Cephei star sample indicates that they all share common properties: they are N-rich targets (e.g., Morel et al. 2008) and, as discussed by Hubrig et al. (2009), their pulsations are dominated by a non-linear dominant radial mode (see also Saesen 2006 for ξ^1 CMa). The presence of a magnetic field might consequently play an important role to explain such a distinct behaviour of magnetic β Cephei stars. More precisely, chemical abundance anomalies are commonly believed to be due to radiatively-driven microscopic diffusion in stars rotating sufficiently slowly to allow such a process to be effective. However, we need an additional clue to account for the fact that both normal and nitrogen-enriched slowly rotating stars are observed. The presence of a magnetic field is a very plausible explanation, as it can add to the stability of the atmosphere, allowing diffusion processes to occur (Michaud 1970). On the other hand, among the studied stars, apart from the star 15 CMa with rather low $v_{\text{eq}} = 40 \pm 6 \text{ km s}^{-1}$, the other three magnetic pulsating stars rotate much faster up to $v_{\text{eq}} = 165 \pm 21 \text{ km s}^{-1}$ for ξ^1 CMa with the strongest magnetic field, indicating that these stars are not truly slowly rotating stars, but seen close to pole-on. Obviously, the topic of mixing signatures is not understood theoretically yet and more computational work as well as future additional observational validation of our results are needed to understand the link between the presence of a magnetic field, rotation, pulsating characteristics, and abundance peculiarities.

T.M. acknowledges financial support from Belspo for contract PRODEX GAIA-DPAC.

REFERENCES

- Babcock, H. W., 1958, ApJS, 3, 141
- Briquet, M., Hubrig, S., De Cat, P., Aerts, C., North, P., & Schöller, M., 2007, A&A, 466, 269
- Diaz-Cordovés, J., Claret, A., & Gimenez, A. 1995, A&AS, 110, 329
- Hasan, S. S., Zahn, J.-P., & Christensen-Dalsgaard, J. 2005, A&A, 444, L29

- Henrichs, H. F., Neiner, C., Hubert, A. M., Floquet, M., & the MuSiCoS Team 2000, in ASP Conf. Ser. Vol. 214, *The Be Phenomenon in Early-Type Stars*, eds. M.A. Smith & H.F. Henrichs, 372
- Hubrig, S., Kurtz, D. W., Bagnulo, S., Szeifert, T., Schöller, M., Mathys, G., & Dziembowski, W. A. 2004a, *A&A*, 415, 661
- Hubrig, S., Szeifert, T., Schöller, M., Mathys, G., & Kurtz, D. W. 2004b, *A&A*, 415, 685
- Hubrig, S., Briquet, M., Schöller, M., De Cat, P., Mathys, G., & Aerts, C. 2006, *MNRAS*, 369, L61
- Hubrig, S., North, P., & Schöller, M., 2007, *AN* 328, 475
- Hubrig, S., Briquet, M., De Cat, P., Schöller, M., Morel, T., & Ilyin, I. 2009, *AN*, 330, 317
- Ilyin, I. V. 2000, *Numerical methods for the data analysis*, Manuscript, 132 pages
- Lefever, K., Puls, J., Morel, T., Aerts, C., Decin, L., & Briquet, M. 2010, *A&A*, 515, A74
- Michaud, G. 1970, *ApJ*, 160, 641
- Morel, T., Hubrig, S., & Briquet, M. 2008, *A&A*, 481, 453
- Neiner, C., Geers, V.C., Henrichs, H.F., Floquet, M., Frémat, Y., Hubert, A.-M., Preuss, O., & Wiersema, K. 2003a, *A&A*, 406, 1019
- Neiner, C., et al. 2003b, *A&A*, 411, 565
- Press, W. H., Teukolsky, S. A., Vetterling, W. T., & Flannery, B. P. 1992, *Numerical Recipes*, 2nd ed. (Cambridge University Press: Cambridge)
- Preston, G. W. 1969, *ApJ*, 156, 967
- Rudy, R. J., & Kemp, J. C., 1978, *MNRAS*, 183, 595
- Saesen, S., Briquet, M., & Aerts, C. 2006, *Comm. in Asteroseismology*, 147, 109
- Seber, G. A. F. 1977, *Linear Regression Analysis* (Wiley: New York)
- Shibahashi, H., & Aerts, C., 2000, *ApJ*, 531, L143
- Shobbrook, R. R., Handler, G., Lorenz, D., & Mogorosi, D. 2006, *MNRAS*, 369, 171
- Stankov, A., & Handler, G. 2005, *ApJS*, 158, 193

Tuominen, I., Ilyin, I., & Petrov, P. 1999, in *Astrophysics with the NOT*, eds. H. Karttunen & V. Piirola, University of Turku, Tuorla Observatory, 47